



# Effect of the Lüders plateau on ductile fracture with MBL model

Shengwen Tu<sup>a</sup>, Xiaobo Ren<sup>b</sup>, Jianying He<sup>a</sup>, Zhiliang Zhang<sup>a,\*</sup>

<sup>a</sup> Department of Structural Engineering, Norwegian University of Science and Technology (NTNU), Trondheim, 7491, Norway

<sup>b</sup> SINTEF Industry, Trondheim, 7465, Norway

## ARTICLE INFO

### Keywords:

Lüders plateau  
Ductile fracture  
Stress triaxiality  
Gurson damage model  
MBL model

## ABSTRACT

In this study, the effect of Lüders plateau on the ductile crack growth resistance has been investigated with the Gurson damage model and the modified boundary layer (MBL) model, under mode I plane strain condition. The Lüders plateau is modeled as horizontal by keeping the plateau stress equaling to the yield stress. A family of Lüders elongations ranging from 0 to 5% has been considered. The remote boundary condition of the MBL model is governed by the elastic  $K$ -field and  $T$ -stress. Numerical results show that the existence of the Lüders plateau on the stress-strain curve reduces the ductile crack growth resistance. The degree of reduction depends on the scale of the Lüders elongation. The crack tip stress field analysis indicates that the existence of the Lüders plateau varies the crack tip stress triaxiality distribution and the magnitude. It is also found that the size of plastic zone ahead of the crack tip is reduced, compared with the reference case for material without Lüders plateau. It is demonstrated that the effect of Lüders plateau on ductile crack growth is more significant at lower  $T$ -stress or for materials with higher toughness. The dependence of the initial void volume fraction and the  $T$ -stress on the ductile crack growth resistance are alleviated when the Lüders elongation is large.

## 1. Introduction

Mechanical properties of structural materials play a very important role in structural integrity assessment. For some metallic materials, a so-called Lüders plateau can be observed on the stress-strain curve just after the elastic regime. Lüders banding, a material instability associated with unpinning of dislocations from nitrogen and carbon atmospheres (Cottrell and Bilby, 1949; Johnston and Gilman, 1959; Hall, 2012), was first reported by Guillaume Piolet and later W. Lüders. For some seamless pipeline steels used in offshore reeling installation and some structural steels studied for Arctic applications, the Lüders plateau is observed with the value of Lüders elongation in the range of 1–3% at room temperatures. Experimental investigations performed by Tsuchida et al. (2006) demonstrated that for materials exhibiting Lüders plateau, the Lüders elongation increased with the decrease of temperatures and the ferrite grain size. The Lüders elongation may increase up to 7% for specimens with ferrite grain size of  $1.1 \mu\text{m}$  tested at  $-63^\circ\text{C}$  at the initial strain rate of  $3.3 \times 10^{-4}\text{s}^{-1}$ . The temperature dependence on the Lüders elongation has also been reported by Ren et al. (2015).

The existence of Lüders plateau on the stress-strain curves may influence the bending behavior of steel tubes and the ductile fracture response of pipeline steels. Hallai and Kyriakides, 2011a, 2011b

performed bending tests on Carbon steel (CS) with the ratio of nominal diameter ( $D$ ) and the wall thickness ( $t$ ),  $D/t$ , in the range of 14.7–33.2. The tubes were firstly heat-treated in a vacuum furnace to reappear Lüders plateau. After heat treatment the tubes developed Lüders strain in the range of 1.8–2.7%, with yield stress varying from 220 to 358 MPa. The tubes were then bent to collapse in a four-point bending facility. They found that the Lüders plateau influenced the curvature distribution on the tension and compression sides, coupled with  $D/t$ . For relatively lower  $D/t$  and/or short Lüders elongation, Lüders bands spread the whole tube and then the tube entered into the hardening regime until collapse. The limit moment instability was not influenced. For higher  $D/t$  tubes and/or longer Lüders elongation, the propagation of Lüders bands was terminated by localized collapse, when a critical length was Lüders deformed while the rest of the tube was essentially undeformed. By simplifying the Lüders plateau as horizontal and keeping the plateau stress equaling to the yield stress, some numerical analyses were performed to study the effect of Lüders plateau on the tensile strain capacity (Tang et al., 2014) or the crack driving force (Dahl et al., 2018). Tang et al. (2014) investigated the effect of Lüders plateau on the tensile strain capacity of welded pipelines and found out that the relatively small Lüders elongation can cause a relative increase to tensile capacity while large Lüders elongation can cause a relative decrease. Tkaczyk et al. (2009) performed numerical analyses to study

\* Corresponding author.

E-mail address: [zhiliang.zhang@ntnu.no](mailto:zhiliang.zhang@ntnu.no) (Z. Zhang).

<https://doi.org/10.1016/j.euromechsol.2019.103840>

Received 14 May 2019; Received in revised form 1 August 2019; Accepted 11 August 2019

Available online 14 August 2019

0997-7538/ © 2019 The Authors. Published by Elsevier Masson SAS. This is an open access article under the CC BY-NC-ND license (<http://creativecommons.org/licenses/by-nc-nd/4.0/>).

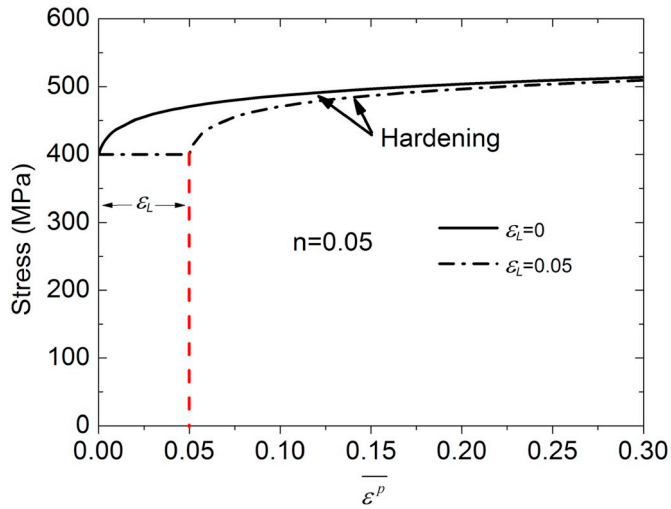


Fig. 1. Illustration of the flow stress-strain curve with Lüders plateau used in this study.

the effect of Lüders plateau on crack driving force of a X65 pipeline with part circumferential external surface elliptical crack. They found an abrupt jump of crack driving force (phrased in terms of J-integral) under tensile loading at the yield strain on the J-strain curve. Dahl et al. (2018) investigated the effect of Lüders plateau on crack driving force (phrased in terms of crack tip opening displacement) with single edge notched tensile (SENT) specimen. They found out that the existence of Lüders plateau intensified the crack driving force and large Lüders elongation corresponded to large increment. Nourpanah and Taheri (2011) conducted numerical analyses to study the effect of Lüders plateau on fracture response of pipelines subject to plastic bending. They reported that the existence of Lüders plateau decreased the constraint ahead of the crack tip and elevated the equivalent plastic strain near the crack tip region.

As introduced above, most investigations focused on the effect of Lüders plateau on bending behavior or the crack driving force. The effect of Lüders plateau on the crack growth resistance is not well understood. In this study, we performed numerical analyses with the complete Gurson damage model under mode I plane strain condition to investigate the Lüders plateau influence on ductile crack growth resistance. The modified boundary layer model (MBL) was utilized with the remote boundary condition governed by elastic  $K$ -field and  $T$ -stress. The effect of Lüders plateau on ductile crack growth resistance was studied and discussed by comparing the cases with Lüders plateau and the reference case without Lüders plateau.

## 2. The complete Gurson damage model

It is widely acknowledged that ductile failure in metals is a result of the nucleation, growth and coalescence of microvoids. In the past decades, many damage models have been developed to simulate ductile fracture and to predict ductile crack growth resistance. Among these models, the one, originally proposed by Gurson (1977) and latter modified by Tvergaard and Needleman (Tvergaard, 1981, 1982), is very popular and known as the Gurson–Tvergaard–Needleman (GTN) model. By introducing stress triaxiality and a void volume fraction parameter in the yield function, the GTN model takes into account the hydrostatic stress effect on plastic yielding and has the following form:

$$\varphi(q, \sigma_f, f, \sigma_m) = \frac{q^2}{\sigma_f^2} + 2q_1 f \cosh\left(\frac{3q_2 \sigma_m}{2\sigma_f}\right) - 1 - (q_1 f)^2 = 0 \quad (1)$$

where  $q$  and  $\sigma_m$  are the von Mises stress and the hydrostatic stress.  $\sigma_f$  is the flow stress of the matrix materials and is a function of the

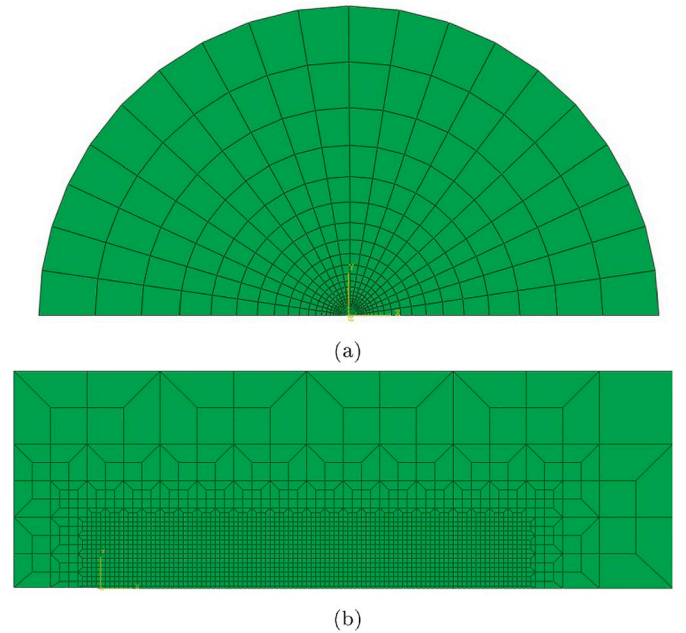


Fig. 2. Modified boundary layer model used for numerical analysis: (a) Global mesh; (b) Local mesh.

equivalent plastic strain,  $\bar{\epsilon}^p$ .  $q_1$  and  $q_2$  are the parameters introduced by Tvergaard, 1981, 1982 and fixed values  $q_1 = 1.5$  and  $q_2 = 1$  are used for all the analyses in present study.  $f$  is the void volume fraction parameter. Due to its robustness in modelling ductile fracture, the GTN model is widely applied in engineering failure analyses and some extended versions have been developed for anisotropy materials (Grange et al., 2000), shear dominated failure (Nahshon and Hutchinson, 2008). Modifications of the GTN model by incorporating void shape effect under loading have been reported by Madou and Leblond in ref. (Madou and Leblond, 2012a, 2012b).

For numerical analyses with the GTN model, the void nucleation model should be determined beforehand (Zhang et al., 2000; Zhang and Niemi, 1994). For the cluster void nucleation model, voids are assumed to be nucleated at the early stage of plastic deformation and the void volume fraction is solely contributed by the void growth while new void nucleation is ignored. This model is suitable for metallic materials containing large inclusion, such as manganese sulfide. For some engineering materials where voids are nucleated from carbides or

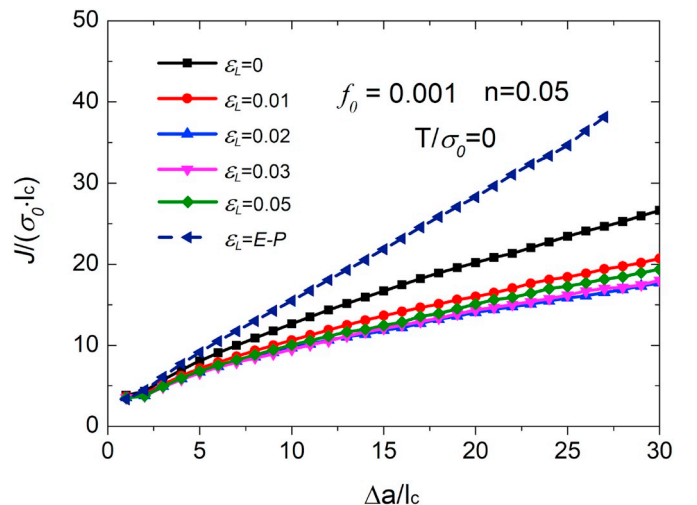


Fig. 3. Normalized resistance curves in terms of J-integral for materials with various Lüders elongations.

intermetallic phase, a continuous void nucleation model which links the amount of voids nucleated to the equivalent plastic strain increment may be applied. In present study, only the cluster nucleation model is considered. Due to the incompressible nature of the matrix material, the void volume fraction increment can be expressed as:

$$df_{growth} = (1 - f)d\epsilon^P : \mathbf{I} \quad (2)$$

where  $d\epsilon^P$  is the plastic strain increment tensor and  $\mathbf{I}$  is the second-order unit tensor. As void volume grows continuously, void coalescence will occur in the following. Tvergaard and Needleman (1984) proposed a function to simulate the effect of void coalescence on the load carrying capacity of the matrix material:

$$f^* = \begin{cases} f & \text{for } f \leq f_c \\ f_c + \frac{f_u - f_c}{f_f - f_c}(f - f_c) & \text{for } f > f_c \end{cases} \quad (3)$$

where  $f_u^* = 1/q_1$ . In Eq. (3), void coalescence takes place when a critical volume fraction,  $f_c$ , is reached. When the condition  $f > f_c$  is satisfied,  $f^*$  replaces  $f$  in Eq. (1). With the void volume fraction increasing up to  $f_f$ , void coalescence is finished. Meanwhile, the element is assumed to lose load carrying capacity and cracks are supposed to propagate. An empirical equation,  $f_f = 0.2 + 2f_0$  is used in this study (Zhang et al., 2000).

For some applications of the GTN model,  $f_c$  was determined arbitrarily or empirically, solely taking into account the homogenous deformation mode (Han et al., 2014). As a results, different pairs of  $(f_0, f_c)$  give identical predictions. Thomason (Thomason and Thomason) proposed that the localized deformation mode (which can be described by the so-called plastic limit load model) of void coalescence should be considered. The competition between the homogeneous deformation mode and the localized deformation mode determines void coalescence. In the early state, voids are so small that the stress required for localized deformation is much higher than that for homogeneous deformation and the latter one is followed. As plastic deformation increases and void grows, the stress required for localized deformation decreases. When the stress for localized deformation is equal to the stress for homogeneous deformation, localized deformation becomes dominate and the void coalescence will occur. By introducing the competition of homogeneous void growth model and the Thomason's plastic limit load model, a so-called "complete Gurson model" which can not only simulate the void nucleation and growth, but also the coalescence process without a pre-selected critical void volume fraction was developed and implemented into Abaqus using a user subroutine UMAT by Zhang (Zhang et al., 2000; Zhang and Niemi, 1994). "Complete" means the model can capture the void nucleation, growth and coalescence

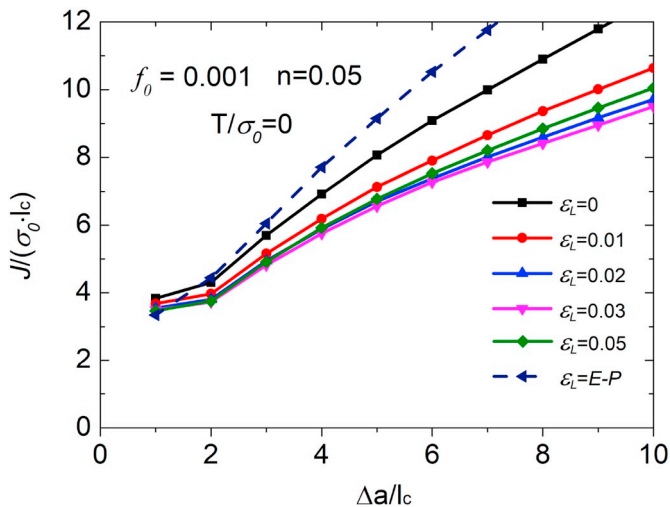
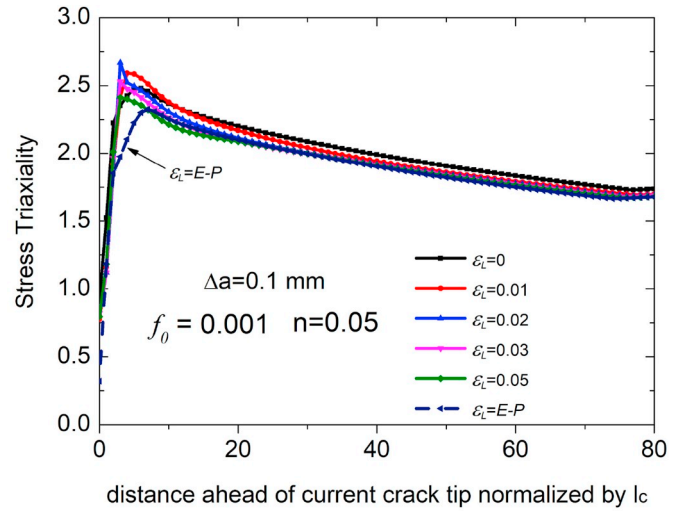
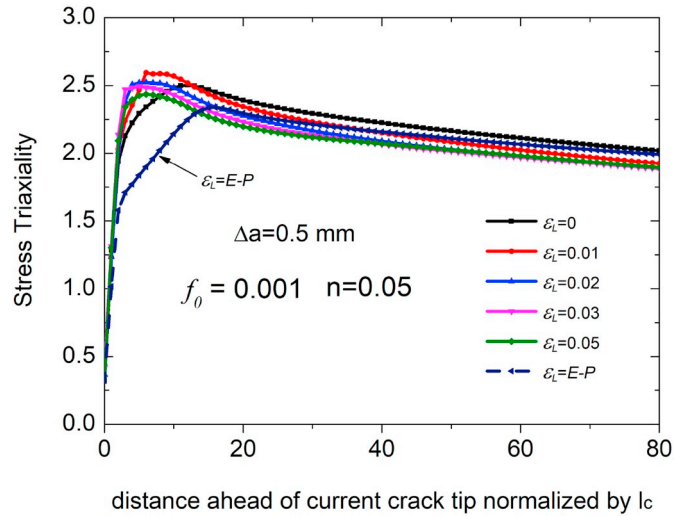


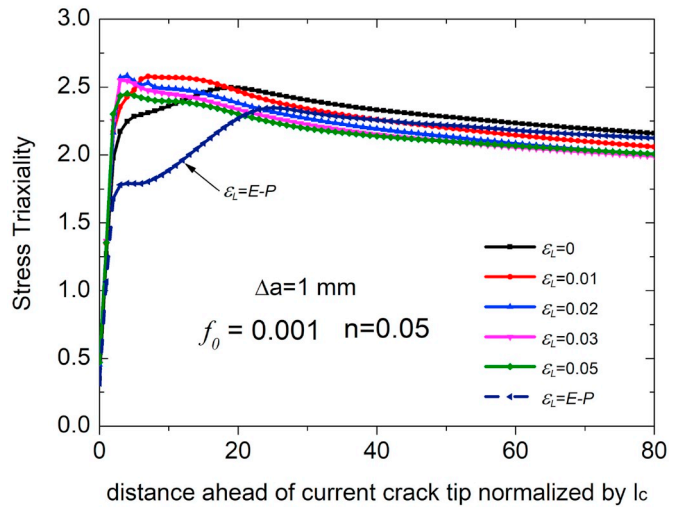
Fig. 4. Normalized resistance curves for materials with various Lüders elongations at short crack advance.



(a)



(b)



(c)

Fig. 5. Stress triaxiality distribution ahead of current crack tip: (a)  $\Delta a = 0.1\text{mm}$ ; (b)  $\Delta a = 0.5\text{mm}$ ; (c)  $\Delta a = 1\text{mm}$ .

automatically once the nucleation parameters are given, and no parameter such as the critical void volume fraction should be determined beforehand. It should be pointed out that the critical void volume fraction in the GTN model is sometimes chosen arbitrary in many studies. However, the “complete Gurson model” determines the critical void volume fraction automatically and physically, since void coalescence is a result of the competition of stresses required for global deformation and the localized deformation. The so-called complete Gurson model is used in this work to study the effect of the Lüders plateau on ductile crack growth. It may be interesting to verify whether the Thomason criterion is accurate for the materials with Lüders plateau, since only smooth stress-strain curve was considered in the past studies. However, this is out of the scope of the present study and will not be discussed below.

### 3. Numerical procedure

#### 3.1. Materials properties

In this study, the Lüders plateau is assumed to be horizontal and the plateau stress is equal to the yield stress. Flow stress-strain curve of the matrix is described by the following rule:

$$\sigma_f = \begin{cases} \sigma_0 & \text{for } \bar{\varepsilon}^p \leq \varepsilon_L \\ \sigma_0 \left(1 + \frac{\bar{\varepsilon}^p - \varepsilon_L}{\varepsilon_0}\right)^n & \text{for } \bar{\varepsilon}^p > \varepsilon_L \end{cases} \quad (4)$$

where  $\sigma_0$ ,  $\varepsilon_0$  and  $n$  are the yield stress, yield strain and the strain hardening exponent, respectively. For all the analyses,  $\sigma_0 = 400$  MPa,  $\sigma_0/E = 0.002$  and  $\nu = 0.3$  are used.  $E$  is the Young's modulus and  $\nu$  is the Poisson ratio. The elastic part of the materials is simply characterized by the yield stress and the Young's modulus.  $\bar{\varepsilon}^p$  and  $\varepsilon_L$  are the equivalent plastic strain and Lüders elongation. Fig. 1 presents the flow stress-strain curves for  $\varepsilon_L = 0, 0.05$  with  $n = 0.05$ , as an example. When  $\varepsilon_L = 0$ , material enters into strain hardening domain just after the elastic regime and no Lüders behavior is expected.

#### 3.2. Finite element modelling of MBL model

In elastoplastic fracture mechanics, the MBL model was widely used to study the crack tip constraint (O'dowd and Shih, 1991, 1992; Xia and Shih, 1995), the loading path effect (Jin et al., 2017), ductile and cleavage fracture under small scale yielding (Ren et al., 2009, 2010, 2011) in 2 and 3 dimensions. In this work, the MBL model in 2D plane strain condition is chosen to study the Lüders plateau effect on ductile crack growth for mode I fracture under small scale yielding. Due to the symmetry of the MBL model, only the upper-half part of the geometry is modeled and the symmetry boundary constraint is used. The radius of the MBL model is 1000 mm to ensure that the small scale yielding condition is satisfied. The initial crack length is 1000 mm with an initial opening of 0.02 mm. Mesh of the MBL model can be seen in Fig. 2. Close to the crack tip, very fine mesh is applied with the element size of  $0.1 \times 0.1$  mm, see Fig. 2b. A single layer of elements with the size of  $0.1 \times 0.05$  mm are assigned at the symmetric plane where crack is supposed to propagate. In the following context,  $l_c$  refers to the length of the uniformly sized element. Out of the uniform size region, the element size is gradually increased with radial distance from the crack tip. There are 20 sections within angular region from 0 to  $\pi$  along the circumference. 4-node plane strain elements (CPE4) are applied and finite strains are accounted for in all the analyses.

For the MBL model, the load is applied at the outer surface through a displacement field, controlled by stress intensity factor  $K_I$  and  $T$ -stress. Values of displacement components  $u_x$  and  $u_y$  are calculated from the plane strain  $K_I - T$  stress field:

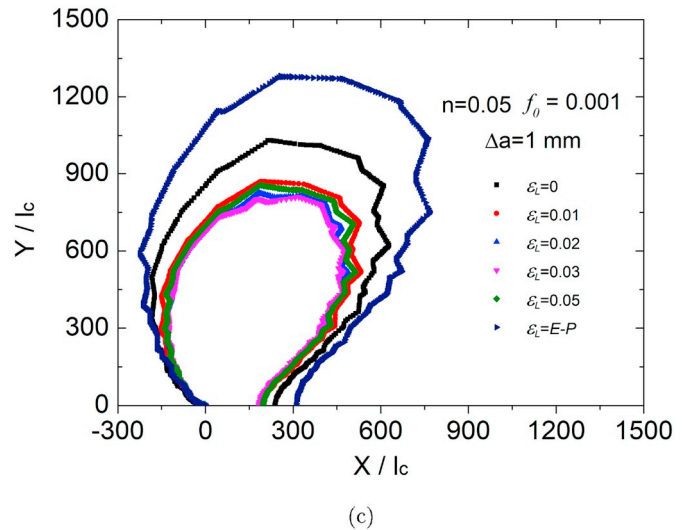
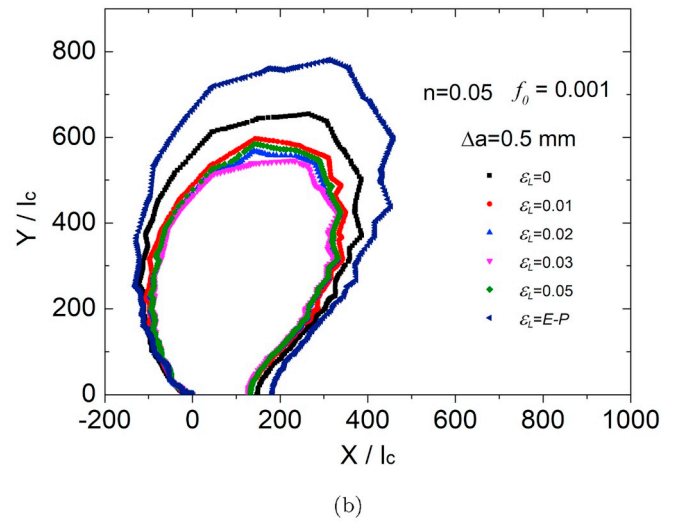
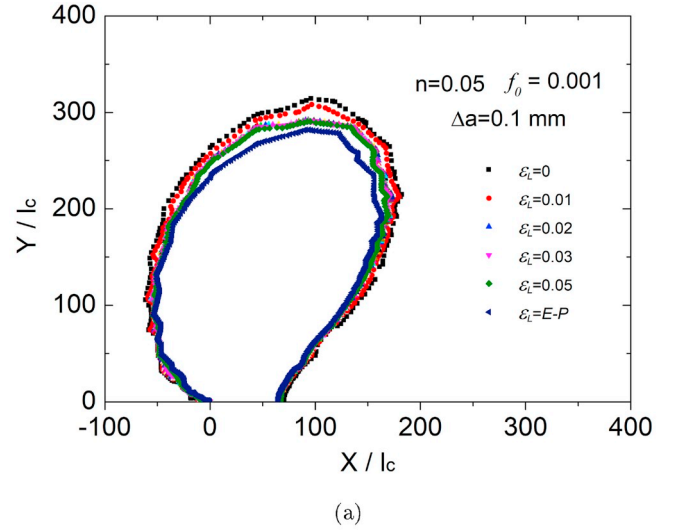


Fig. 6. Plastic zone size at given crack increment: (a)  $\Delta a = 0.1$  mm; (b)  $\Delta a = 0.5$  mm; (c)  $\Delta a = 1$  mm.

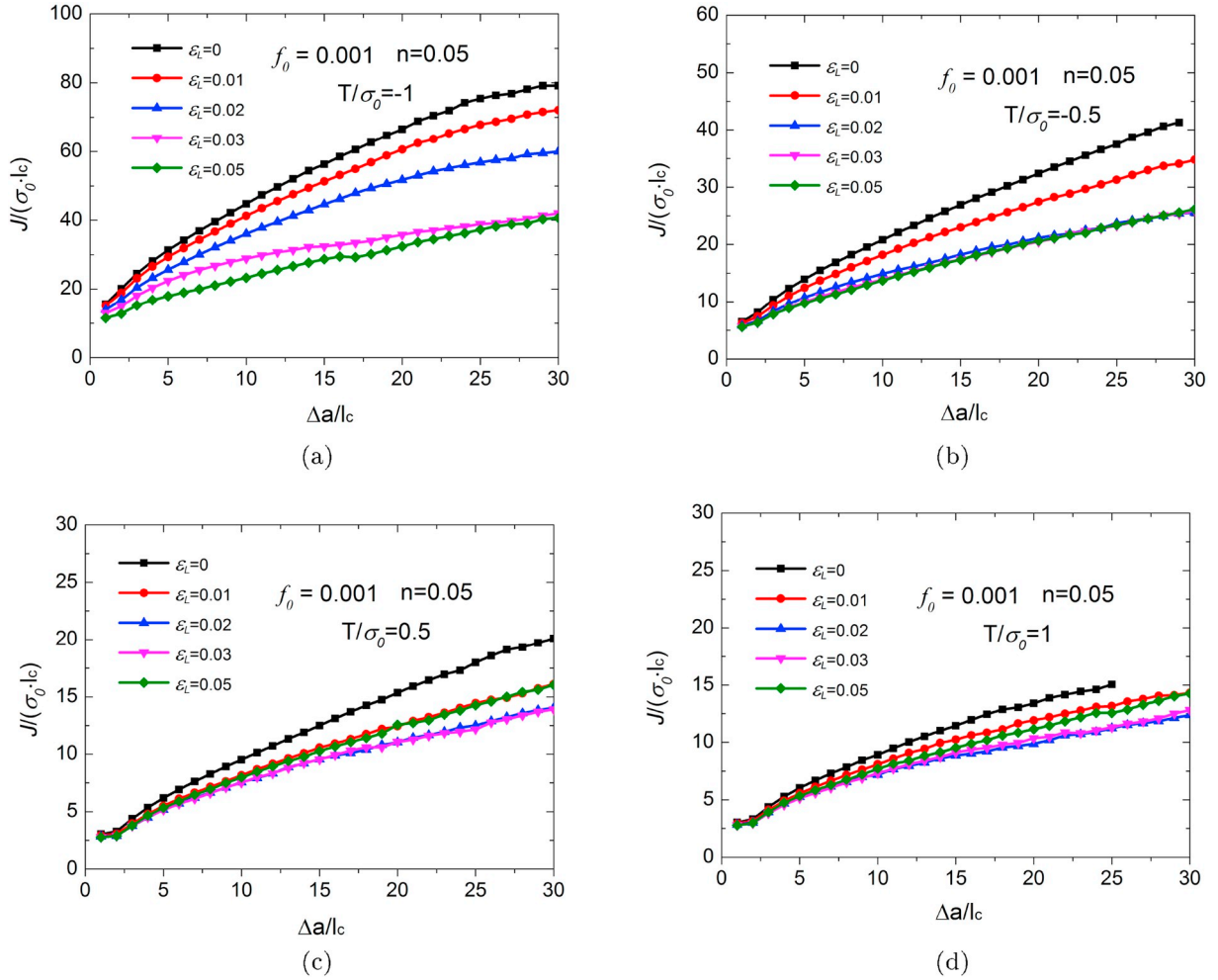


Fig. 7. Resistance curves from MBL model under different  $T$ -stresses: (a)  $T/\sigma_0 = -1$ ; (b)  $T/\sigma_0 = -0.5$ ; (c)  $T/\sigma_0 = 0.5$ ; (d)  $T/\sigma_0 = 1$ .

$$\begin{aligned}
 u_x(r, \theta) &= K_I \frac{1+\nu}{E} \sqrt{\frac{r}{2\pi}} \cos\left(\frac{\theta}{2}\right) (3 - 4\nu - \cos\theta) + T \frac{1-\nu^2}{E} r \cos\theta \\
 u_y(r, \theta) &= K_I \frac{1+\nu}{E} \sqrt{\frac{r}{2\pi}} \sin\left(\frac{\theta}{2}\right) (3 - 4\nu - \cos\theta) - T \frac{\nu(1+\nu)}{E} r \sin\theta
 \end{aligned} \quad (5)$$

where  $K_I = \sqrt{EJ/(1-\nu^2)}$ ,  $J$  is the far-field  $J$ -integral. The displacements are loaded at the out surface of the model proportionally. To obtain crack growth resistance curves in terms of  $J$ -integral in the analyses, domain integral method is used to calculate the  $J$ -integral on the contour close to the out surface. This is due to that close to the crack tip where non-proportional loading may occur,  $J$ -integral displays path-dependence issue. For the complete Gurson model, the crack advances when the void volume fraction at the crack tip reaches  $f_f$ . The crack length is therefore calculated by multiplying the original element length (0.1 mm) by the number of failed elements.

## 4. Results and discussion

### 4.1. Effect of Lüders plateau on ductile crack growth resistance

Resistance curves from numerical analyses with the MBL model are displayed in Fig. 3, with  $T/\sigma_0 = 0$ . The strain hardening exponent and the initial void volume fraction used in Fig. 3 are  $n = 0.05$  and  $f_0 = 0.001$ . The Lüders elongation varies from 0 to 5%. Resistance curve for the elastic – perfectly plastic material is also presented. It is noted that the two limiting cases are considered: material without Lüders elongation ( $\varepsilon_L = 0$ ) and the elastic – perfectly plastic material (legended as  $\varepsilon_L = E - P$  in the following text).  $J$ -integral in Fig. 3 is normalized by

the product of  $\sigma_0$  and  $l_c$  while the crack growth is normalized by  $l_c$ . It can be seen that resistance curves for materials with Lüders plateau are lower than the reference case for  $\varepsilon_L = 0$ . As expected, the resistance curve for the elastic – perfectly plastic material is higher than other cases in Fig. 3. It can also be observed in Fig. 3 that the resistance curves decrease with the increasing  $\varepsilon_L$  when the Lüders elongation is very small. As  $\varepsilon_L$  increases to 0.02, the corresponding resistance curve appears to be the lowest in Fig. 3 and almost overlaps to the resistance curve for  $\varepsilon_L = 0.03$ . After reaching the lowest one, resistance curve shifts up with the increase of the Lüders elongation gradually. For  $\varepsilon_L = 0.05$ , the resistance curve is slightly higher than the lowest one but still lower than that for  $\varepsilon_L = 0$ . It may be expected that for larger Lüders elongation, the resistance curve will shift up and even be higher than the reference case for  $\varepsilon_L = 0$ , see the resistance curve for the elastic – perfectly plastic material. However, for most engineering metallic materials exhibiting Lüders plateau, Lüders elongation is usually smaller than 5%, though slightly increase with temperature decrease.

Resistance curves in Fig. 3 are replotted with  $\Delta a/l_c$  up to 10 and are presented in Fig. 4. It can be seen that the toughness at crack initiation ( $\Delta a = 0.1\text{mm}$ ) decreases slightly with the increase of the Lüders elongation. The reduction of the crack initiation toughness due to the Lüders elongation has also been reported by Nourpanah and Taheri (2011). For the elastic – perfectly plastic material, the toughness at crack initiation is the lowest. After crack initiation, the resistance curve rises rapidly and becomes the highest. For  $\varepsilon_L$  increasing up to 0.03, the resistance curves shift down uniformly. The resistance curve for  $\varepsilon_L = 0.05$  is the lowest after crack initiation. Up to  $\Delta a/l_c = 3$ , it presents

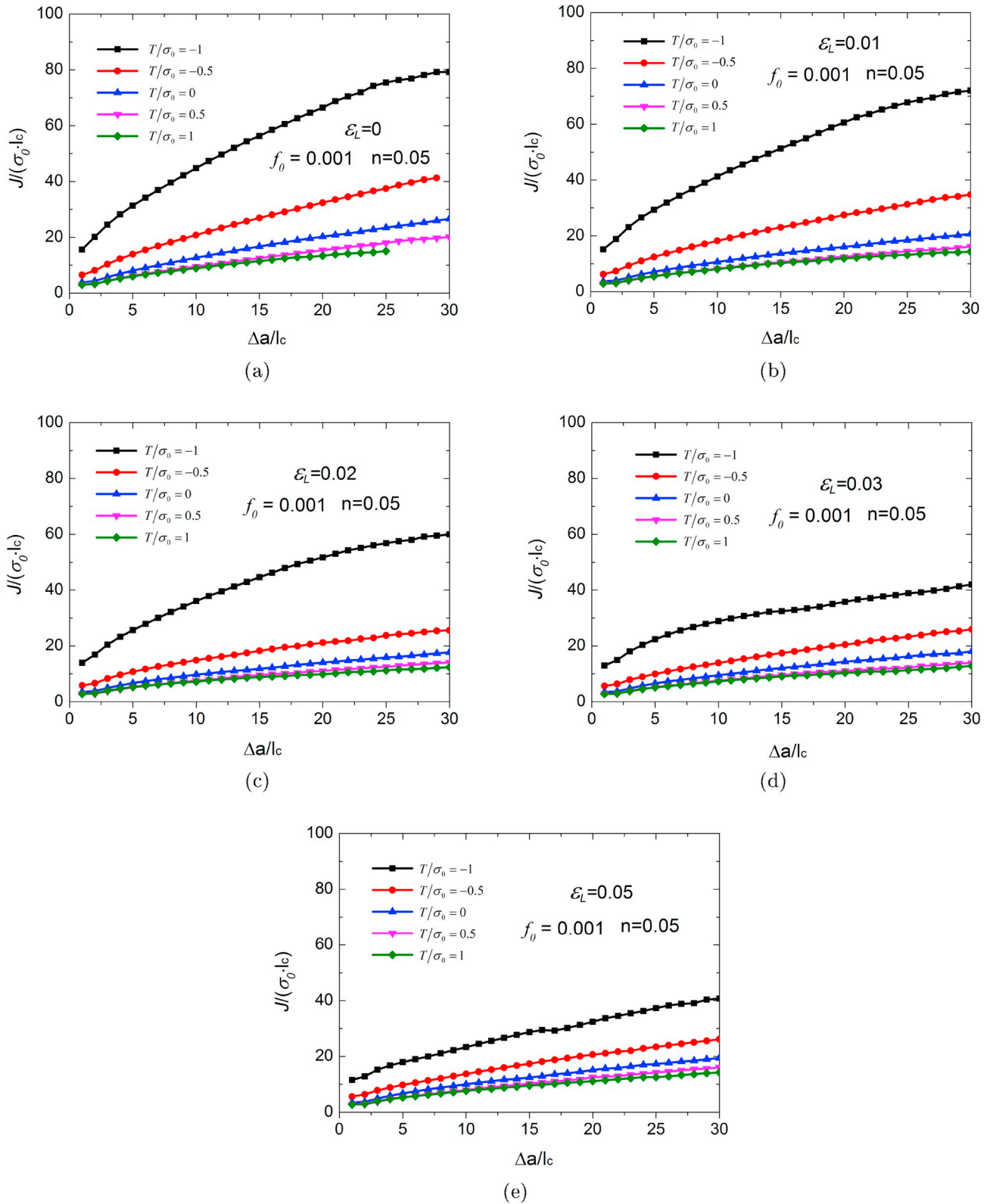


**Fig. 8.** Resistance curves dependence on  $T$  stress for materials with the same Lüders elongation: (a)  $\varepsilon_L = 0$ ; (b)  $\varepsilon_L = 0.01$ ; (c)  $\varepsilon_L = 0.02$ ; (d)  $\varepsilon_L = 0.03$ ; (e)  $\varepsilon_L = 0.05$ .

to be higher than the corresponding resistance curves for  $\varepsilon_L = 0.02$  and  $\varepsilon_L = 0.03$ . Though the gap between the resistance curves for  $\varepsilon_L = 0.02$  and  $\varepsilon_L = 0.03$  is very small, it can still be observed that resistance curve for  $\varepsilon_L = 0.03$  is slightly lower than that for  $\varepsilon_L = 0.02$  in Fig. 4. While in Fig. 3, resistance curve for  $\varepsilon_L = 0.03$  is slightly higher than the one for

$\varepsilon_L = 0.02$  when  $\Delta a/l_c \geq 15$ . The resistance curve for  $\varepsilon_L = 0.03$  rises more rapidly than  $\varepsilon_L = 0.02$  with crack propagation.

Resistance curves in Figs. 3 and 4 indicate that the introduction of Lüders plateau on the stress-strain curve reduces materials' ability to resist crack propagation. To understand the effect of Lüders plateau on

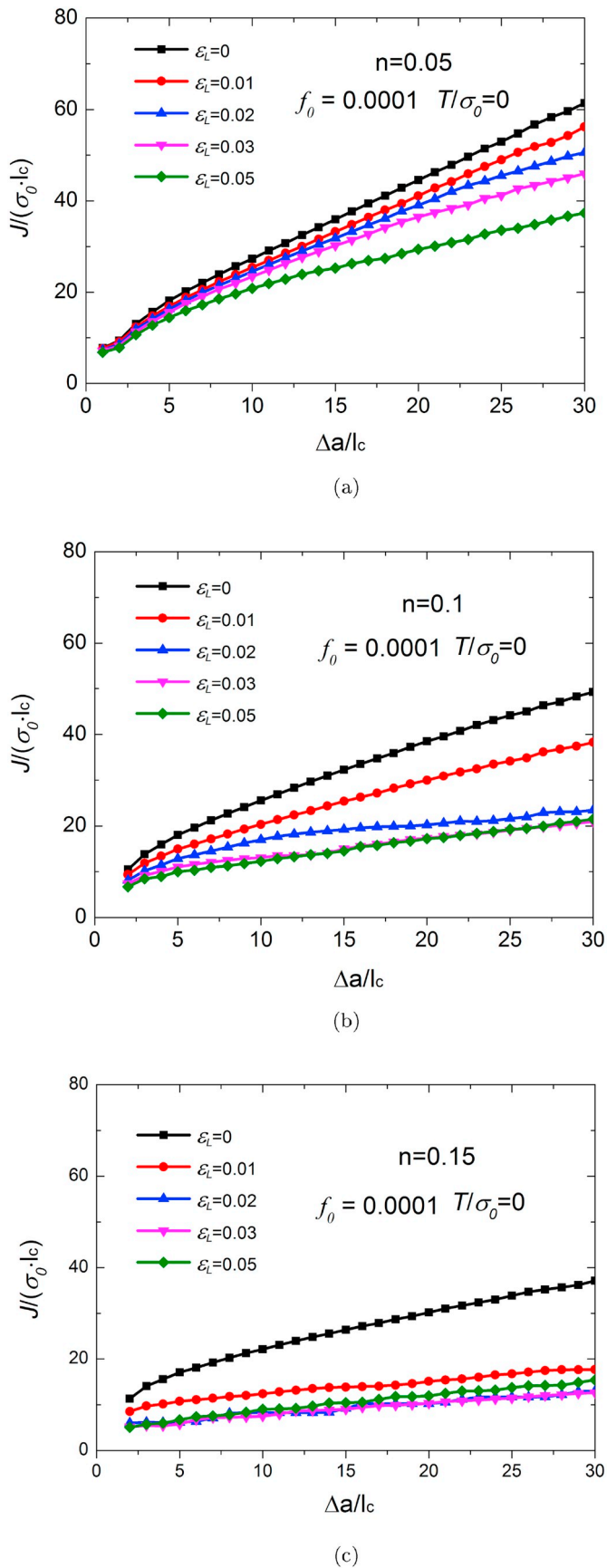


Fig. 9. Effect of Lüders plateau on resistance curves for materials with different strain hardening: (a)  $n = 0.05$ ; (b)  $n = 0.1$ ; (c)  $n = 0.15$ .

the ductile crack growth resistance curves, the stress triaxiality (ratio of hydrostatic stress over the von Mises equivalent stress) ahead of the crack tip corresponding to  $\Delta a = 0.1, 0.5$  and  $1\text{mm}$  are presented in Fig. 5, as a function of the distance from the current crack tip. In Fig. 5a, the stress triaxiality distribution differs to each other. For materials with Lüders plateau, the maximum stress triaxiality is higher than the reference case for  $\varepsilon_L = 0$ , except  $\varepsilon_L = 0.05$ . This indicates that small Lüders elongations elevate the magnitude of stress triaxiality ahead of the crack tip; larger Lüders elongations in return reduces the magnitude of stress triaxiality. For materials under higher stress triaxiality, damage evolution happens at relatively early stage which will result in smaller fracture strain. Therefore, small Lüders elongations accelerate the damage accumulation, which as a result facilitate the crack propagation. It can also be observed that the distance corresponding to the maximum stress triaxiality reduces for materials with Lüders plateau, compared with  $\varepsilon_L = 0$ . It means that void volume fraction ahead of the crack tip for materials with Lüders plateau will increase more quickly and less energy is required for crack propagation. The distribution and magnitude in Fig. 5a well explain the decrease of crack initiation toughness ( $\Delta a = 0.1\text{mm}$ ) in Fig. 4, except  $\varepsilon_L = 0.05$  and the elastic – perfectly plastic material. In Fig. 5b and c, the maximum stress triaxiality for  $\varepsilon_L = 0.01, 0.02, 0.03$  are slightly higher and locate more closer to the crack tip than the case  $\varepsilon_L = 0$ . Correspondingly, lower resistance curves can be seen in Figs. 3–4. Though the maximum stress triaxiality for  $\varepsilon_L = 0.01$  is slightly larger than  $\varepsilon_L = 0.02$  and  $0.03$ , the corresponding distance to the maximum stress triaxiality is longer and higher resistance curve is obtained. For  $\varepsilon_L = 0.05$ , the maximum stress triaxiality is lower than  $\varepsilon_L = 0.02$  and  $0.03$ , higher resistance curve can be expected and are seen in Fig. 3. The stress triaxiality ahead of the current crack tip for the elastic – perfectly plastic material is the lowest and the maximum stress triaxiality locates further than other cases. As a result, the resistance curve for the elastic – perfectly plastic material  $\varepsilon_L = E - P$  is the highest in Fig. 3 after crack initiation.

The plastic zone size for  $\bar{\varepsilon}^P \geq 0.01\%$  at  $\Delta a = 0.1, 0.5$  and  $1\text{mm}$  are presented in Fig. 6. The plastic zone size for a given material increases with crack growth. For  $\Delta a = 0.1\text{mm}$  in Fig. 6a, the plastic zone size decreases with the increase of Lüders elongation. It can be seen that the plastic zone size for the elastic – perfectly plastic material is the smallest. This well explains the reduction of crack initiation toughness in Fig. 4: less energy is required at crack initiation for crack tip exhibiting smaller plastic zone size. For  $\Delta a = 0.5$  and  $1\text{mm}$ , the plastic zone size reduces with the increase of Lüders elongation, up to  $\varepsilon_L = 0.03$ . For  $\varepsilon_L = 0.05$ , the plastic zone size is larger than that for  $\varepsilon_L = 0.02$  and smaller than  $\varepsilon_L = 0.01$ . Correspondingly, resistance curve for  $\varepsilon_L = 0.05$  locates between the two cases in Fig. 3. The plastic zone size for all the materials with Lüders plateau is smaller than the reference case for  $\varepsilon_L = 0$  and the resistance curves are lower. For the elastic – perfectly plastic material, the plastic zone size is the maximum and higher resistance is seen in Fig. 3. The plastic zone size in Fig. 6b and c again well explain the trend transition of resistance curves in Fig. 3. The existence of Lüders plateau reduces the plastic zone size at the crack tip and lowers down the materials' ability to resist ductile crack growth, compared to the case for material without Lüders plateau.

#### 4.2. Effect of Lüders plateau on ductile crack growth under different $T/\sigma_0$

Ductile crack growth depends significantly on the crack tip constraint. For the MBL model, constraint at the crack tip can be controlled by introducing the  $T$ -stress. Previous studies on the effect of  $T$ -stress on ductile crack growth shows that negative  $T$ -stress (low constraint) rises the resistance curve rapidly while positive  $T$ -stress (high constraint) lowers down fracture resistance (Zhang et al., 2000). In this study, the effect of Lüders plateau on ductile crack growth with  $T/\sigma_0 = -1, -0.5, 0.5$  and  $1$  is investigated. The  $T$ -stress is loaded at the MBL model out surface firstly and the  $K$ -field is applied in the following. The initial void volume fraction is fixed to be  $0.1\%$  and the hardening exponent

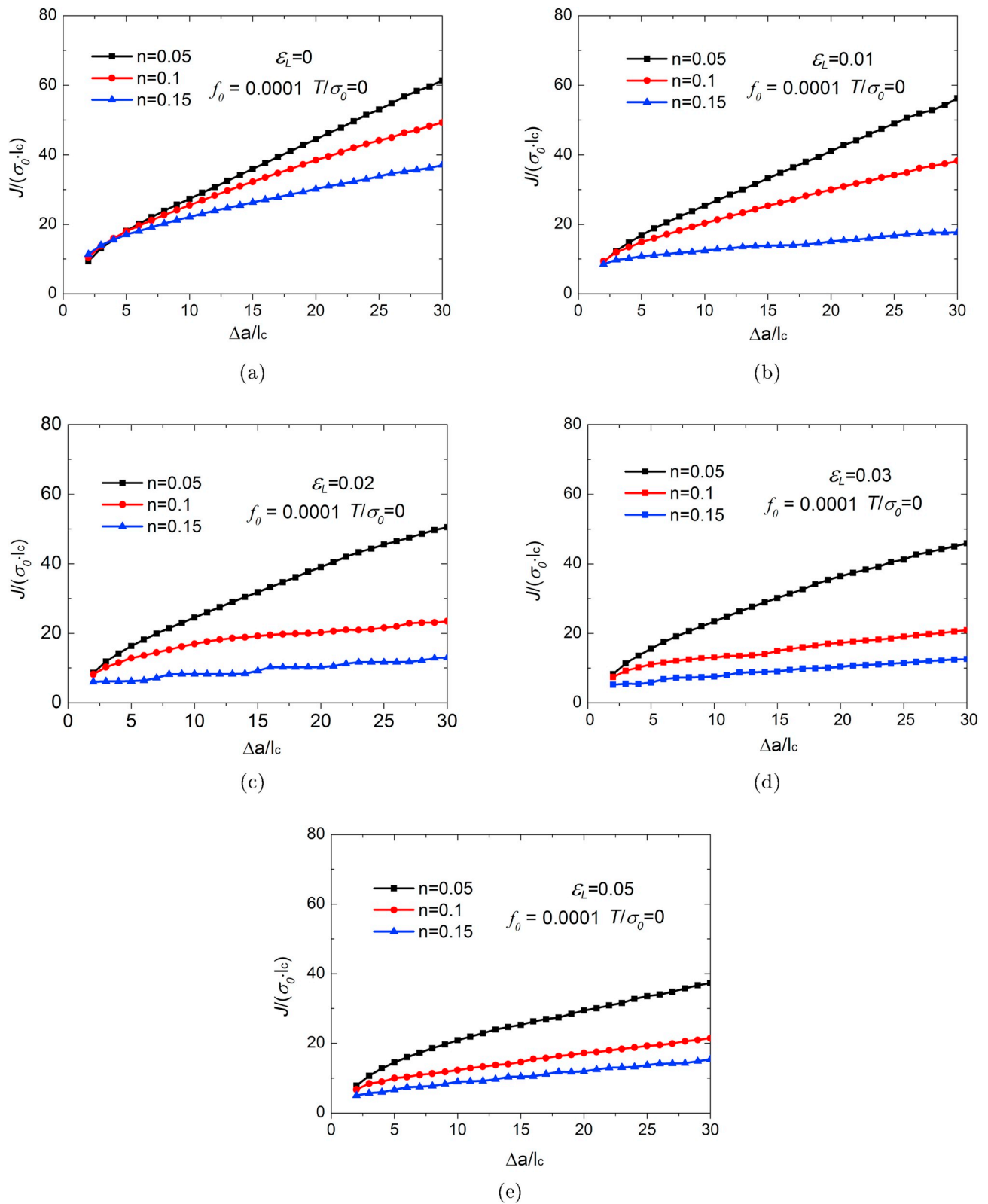


**Fig. 10.** Resistance curves dependence on strain hardening for materials with the same Lüders elongation: (a)  $\epsilon_L = 0$ ; (b)  $\epsilon_L = 0.01$ ; (c)  $\epsilon_L = 0.02$ ; (d)  $\epsilon_L = 0.03$ ; (e)  $\epsilon_L = 0.05$ .

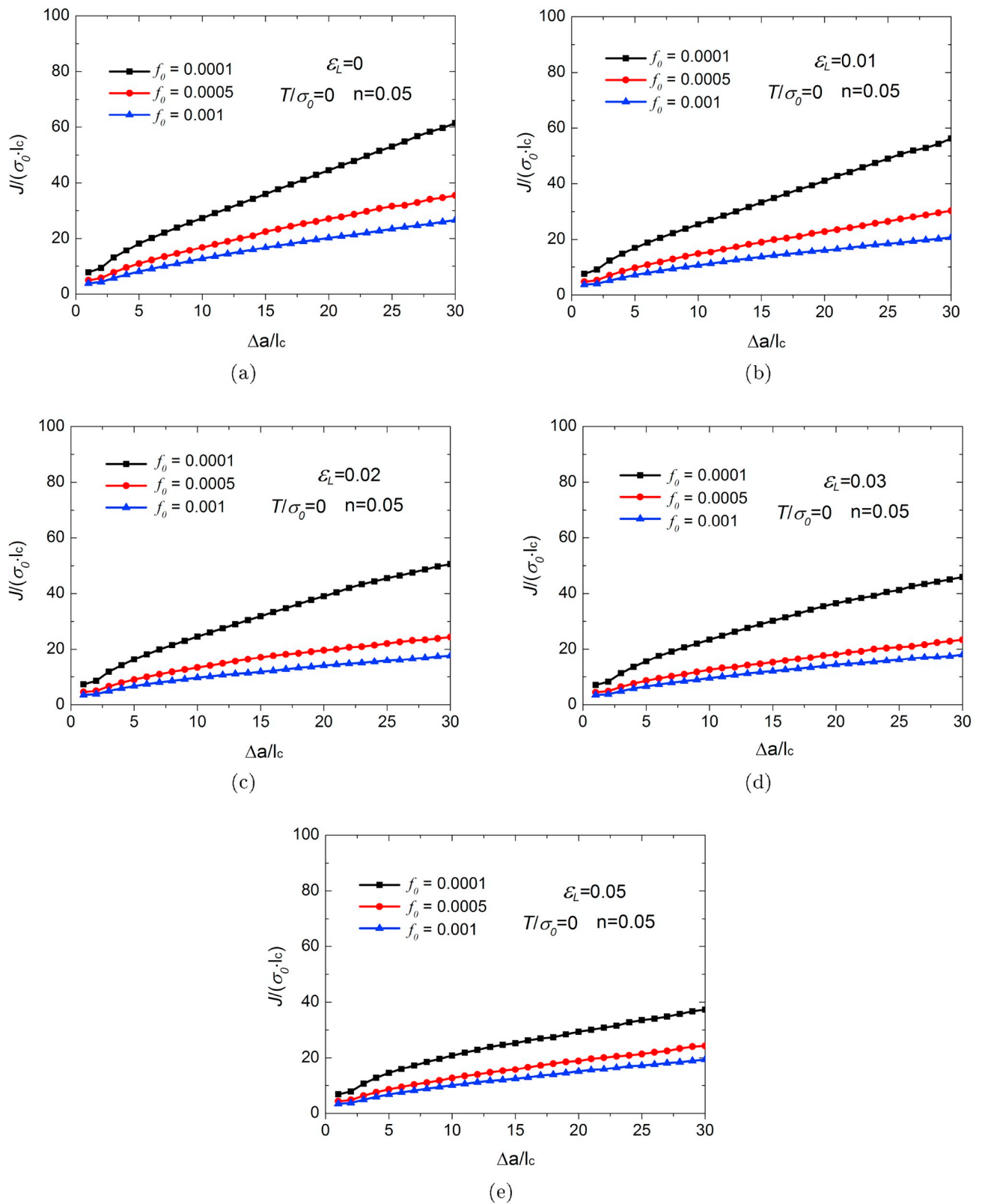


**Fig. 11.** Resistance curves dependence on the initial void volume fraction for materials with the same Lüders elongation: (a)  $\epsilon_L = 0$ ; (b)  $\epsilon_L = 0.01$ ; (c)  $\epsilon_L = 0.02$ ; (d)  $\epsilon_L = 0.03$ ; (e)  $\epsilon_L = 0.05$ .

$n = 0.05$  is considered. Normalized resistance curves are displayed in Fig. 7. It can be seen that for different  $T/\sigma_0$ , materials with  $\varepsilon_L = 0$  presents the highest fracture resistance. The introduction of Lüders plateau reduces the crack growth resistance curves, for all the constraint levels considered in this section. In Fig. 7a,  $T/\sigma_0 = -1$ , the resistance curves shift down uniformly with the increases of Lüders elongation and the one corresponding to  $\varepsilon_L = 0.05$  is the lowest. For  $T/\sigma_0 = 1$  in Fig. 7d, similar findings in Fig. 3 can be seen. Compared with the subfigures in Fig. 7, the gap between the highest resistance curve and the lowest one in each subfigure decreases with the increase of  $T/\sigma_0$ . It is demonstrated that the effect of Lüders plateau on ductile crack growth resistance is more significant under low constraint.

Resistance curves in Figs. 4 and 7 are then regrouped by Lüders elongation and are presented in Fig. 8. As expected, resistance curves lower down with the increase of  $T/\sigma_0$ , for materials with the same Lüders elongation. In Fig. 8a, the resistance curves under negative  $T$ -stress rises rapidly while the reduction of fracture resistance under positive  $T$ -stress is relative minor in Fig. 8d. With the increases of Lüders elongation, the gap between the highest and lowest resistance curves decreases gradually. Fig. 8 shows that the Lüders plateau reduce the  $T$ -stress dependence on ductile crack growth resistance. The reduction becomes more pronounced as Lüders elongation increases.

#### 4.3. Effect of Lüders plateau on ductile crack growth resistance for different hardening exponents

Strain hardening plays an important role on ductile crack growth resistance, though its effect on crack resistance curve is not fully understood. Xia and Shih (1995) reported that increasing strain hardening increases the crack ductile resistance curve rapidly while Østby and Ren (Ren et al., 2010; Østby et al., 2007) demonstrated opposite results. In the section, the effect of Lüders plateau on ductile crack growth resistance is further studied, coupled with strain hardening exponent. The initial void volume fraction is fixed to be 0.01% while the  $T$ -stress is set to be 0. Hardening exponents  $n = 0.05, 0.1$  and  $0.15$  are considered. Corresponding resistance curves are presented in Fig. 9. As can be seen, for materials with Lüders plateau, the resistance curves are lower than the one for  $\varepsilon_L = 0$ . The reduction of fracture resistance (compared with  $\varepsilon_L = 0$ ) increases with strain hardening, for materials with the same Lüders elongation. Especially, for  $n = 0.15$ , the resistance curves for materials with Lüders plateau distribute very close to each other and are much lower than the resistance curve for  $\varepsilon_L = 0$ . Resistance curves in Fig. 9 show that the existence of Lüders plateau reduces ductile crack growth. The reduction of degree also depends on the materials' strain hardening capacity.

Resistance curves in Fig. 9 are regrouped in terms of the Lüders elongation and are presented in Fig. 10. Similar to the findings in Østby and Ren's work (Ren et al., 2010; Østby et al., 2007), materials with lower strain hardening yield higher resistance curves. This is valid for materials with or without Lüders plateau. The gaps between the resistance curves for  $\varepsilon_L = 0.01$  and  $0.02$  are larger than that for  $\varepsilon_L = 0$ . While for  $\varepsilon_L = 0.03$  and  $0.05$ , the gaps tends to contract. In our previous study (Tu et al., 2018), we found that when  $\varepsilon_L = 0.1$ , resistance curves from SENT specimens with  $n = 0.05, 0.1$  and  $0.15$  almost overlapped to each other totally, showing insignificant strain hardening effect. The results in this study and in ref. Tu et al. (2018) may draw the conclusion that the strain hardening effect is more considerable for materials with small Lüders elongation and becomes less significant for larger Lüders elongation.

#### 4.4. Effect of Lüders plateau on ductile crack growth resistance for different initial void volume fraction

Ductile fracture depends significantly on the material toughness. In damage mechanics, materials with smaller initial volume fraction are expected to yield higher crack resistance curves. It may be interesting to

study the effect of Lüders plateau on ductile crack growth resistance, coupled with initial volume fraction. For this consideration, we performed numerical analyses, by keeping all the parameters the same in section 4.1 and only changing the initial void volume fraction parameter,  $f_0$ . In this section, analyses for  $f_0 = 0.0001, 0.0005$  and  $0.001$  are studied and compared.

In Figs. 3 and 9a, all the parameters are the same, except  $f_0$ . The initial volume fraction in Fig. 9a is only 10% for that in Fig. 3. It can be observed that resistance curves in Fig. 9a are much higher than those in Fig. 3, for materials with the same Lüders elongation. The lowest resistance curve in Fig. 9a corresponds to  $\varepsilon_L = 0.05$  while in Fig. 3 the lowest resistance curve yields from materials with  $\varepsilon_L = 0.02$ . It is demonstrated the effect of Lüders plateau on ductile crack growth resistance for materials with higher toughness is even more remarkable. Resistance curves in Figs. 3 and 9a are then grouped by Lüders elongation and are presented in Fig. 11. In addition to the results for cases with  $f_0 = 0.0001$  and  $0.001$ , resistances curves corresponding to  $f_0 = 0.0005$  are also included. Obviously, resistance curves for materials with smaller initial void volume fraction rise rapidly and are much higher than those with larger  $f_0$ . This is valid for all the materials considered in this section, with or without Lüders plateau. It is can also be seen that as the Lüders elongation increase, the gaps between the resistance curves in the subfigures in Fig. 11 decreases. For  $\varepsilon_L = 0.05$ , the gaps are remarkably smaller than those in Fig. 11a for  $\varepsilon_L = 0$ . It can be concluded that the effect of the initial void volume fraction on ductile crack growth is slightly alleviated at large Lüders elongation.

## 5. Concluding remarks

In this study, the effect of Lüders plateau on ductile crack growth resistance was investigated numerically with the MBL model, with the remote boundary condition controlled by  $K$ -field and  $T$ -stress. The finite element analyses were performed in 2D plane strain condition with finite strain theory. The complete Gurson model was utilized to simulate crack propagation. The Lüders plateau was idealized as horizontal and the plateau stress was assumed to be equal to the yield stress. Lüders elongations varying from 0 to 5% were considered. In addition, the effect of Lüders plateau was further investigated, coupled with  $T$ -stress, the strain hardening and the initial void volume fraction. The main findings are listed:

1. The existence of Lüders plateau on stress-strain curve reduces materials' ductile crack growth, for the cases studied. The Lüders plateau modifies the distribution and magnitude of the stress triaxiality ahead of the crack tip. Due to the Lüders plateau, deformation is highly localized at the crack tip and smaller plastic zone size is formed, resulting in lower crack resistance curves.
2. It is found out that the effect of Lüders plateau on ductile crack growth resistance is more significant under lower crack tip constraint (lower  $T$ -stress) and becomes less pronounced at higher  $T$ -stress. The dependence of crack resistance curves on  $T$ -stress is reduced with the increasing Lüders elongation.
3. The effect of strain hardening on ductile crack growth coupled with Lüders plateau was investigated. The results indicate that, similar to the Lüders plateau effect at lower  $T$ -stress, the Lüders plateau effect for materials with lower strain hardening is more significant. Small Lüders elongation enhances the strain hardening effect while large Lüders elongation has the opposite modification.
4. Results from the numerical analyses with different initial void volume fractions show that materials with higher toughness are more sensitive to the Lüders plateau. The effect of initial void volume fraction on ductile crack growth is reduced as Lüders elongation becomes large.

It should be noted that the Lüders plateau in this study is idealized as horizontal. In reality, the Lüders plateau is very complex and the way

of modelling the Lüders behavior in numerical analysis may also be important. Further research can be focused on the way of modelling Lüders plateau on fracture response. In fracture mechanics, the competition between the crack driving force and the crack resistance controls the fracture event. Previous investigations on the effect of Lüders plateau on crack driving force show that the Lüders plateau intensifies the crack driving force (Dahl et al., 2018) while this study indicates that the Lüders plateau reduced ductile crack growth. This two-side effect facilitate ductile fracture for materials exhibiting Lüders plateau. Attention should be paid in engineering application for materials with Lüders plateau.

### Acknowledgement

The Chinese Scholarship Council is greatly acknowledged for the financial support. The authors wish to thank the Research Council of Norway for funding through the Petromaks 2 Programme, Contract No. 228513/E30.

### References

- Cottrell, A.H., Bilby, B., 1949. Dislocation theory of yielding and strain ageing of iron. *Proc. Phys. Soc. Sect. A* 62 (1), 49.
- Dahl, B., Ren, X., Akselsen, O., Nyhus, B., Zhang, Z., 2018. Effect of low temperature tensile properties on crack driving force for arctic applications. *Theor. Appl. Fract. Mech.* 93, 88–96.
- Grange, M., Besson, J., Andrieu, E., 2000. An anisotropic gurson type model to represent the ductile rupture of hydrided zircaloy-4 sheets. *Int. J. Fract.* 105 (3), 273–293.
- Gurson, A.L., 1977. Continuum theory of ductile rupture by void nucleation and growth: Part i—yield criteria and flow rules for porous ductile media. *J. Eng. Mater. Technol.* 99 (1), 2–15.
- Hall, E., 2012. *Yield Point Phenomena in Metals and Alloys*. Springer Science & Business Media.
- Hallai, J.F., Kyriakides, S., 2011a. On the effect of Lüders bands on the bending of steel tubes. part i: Experiments. *Int. J. Solids Struct.* 48 (24), 3275–3284.
- Hallai, J.F., Kyriakides, S., 2011b. On the effect of Lüders bands on the bending of steel tubes. part ii: analysis. *Int. J. Solids Struct.* 48 (24), 3285–3298.
- Han, K., Shuai, J., Deng, X., Kong, L., Zhao, X., Sutton, M., 2014. The effect of constraint on ctod fracture toughness of api x65 steel. *Eng. Fract. Mech.* 124, 167–181.
- Jin, Z., Wang, X., Chen, X., Yu, D., 2017. The effects of nonproportional loading on the elastic-plastic crack-tip fields. *Eng. Fract. Mech.* 169, 18–34.
- Johnston, W.G., Gilman, J.J., 1959. Dislocation velocities, dislocation densities, and plastic flow in lithium fluoride crystals. *J. Appl. Phys.* 30 (2), 129–144.
- Madou, K., Leblond, J.-B., 2012a. A gurson-type criterion for porous ductile solids containing arbitrary ellipsoidal voids—i: limit-analysis of some representative cell. *J. Mech. Phys. Solids* 60 (5), 1020–1036.
- Madou, K., Leblond, J.-B., 2012b. A gurson-type criterion for porous ductile solids containing arbitrary ellipsoidal voids—ii: determination of yield criterion parameters. *J. Mech. Phys. Solids* 60 (5), 1037–1058.
- Nahshon, K., Hutchinson, J., 2008. Modification of the gurson model for shear failure. *Eur. J. Mech. A Solid.* 27 (1), 1–17.
- Nourpanah, N., Taheri, F., 2011. A numerical study on the crack tip constraint of pipelines subject to extreme plastic bending. *Eng. Fract. Mech.* 78 (6), 1201–1217.
- Østby, E., Thaulow, C., Zhang, Z., 2007. Numerical simulations of specimen size and mismatch effects in ductile crack growth—part i: tearing resistance and crack growth paths. *Eng. Fract. Mech.* 74 (11), 1770–1792.
- O’Dowd, N., Shih, C.F., 1991. Family of crack-tip fields characterized by a triaxiality parameter—i. structure of fields. *J. Mech. Phys. Solids* 39 (8), 989–1015.
- O’Dowd, N., Shih, C.F., 1992. Family of crack-tip fields characterized by a triaxiality parameter—ii. fracture applications. *J. Mech. Phys. Solids* 40 (5), 939–963.
- Ren, X., Zhang, Z., Nyhus, B., 2009. Effect of residual stresses on the crack-tip constraint in a modified boundary layer model. *Int. J. Solids Struct.* 46 (13), 2629–2641.
- Ren, X., Zhang, Z., Nyhus, B., 2010. Effect of residual stresses on ductile crack growth resistance. *Eng. Fract. Mech.* 77 (8), 1325–1337.
- Ren, X., Zhang, Z., Nyhus, B., 2011. Effect of residual stress on cleavage fracture toughness by using cohesive zone model. *Fatigue Fract. Eng. Mater. Struct.* 34 (8), 592–603.
- Ren, X., Nordhagen, H.O., Zhang, Z., Akselsen, O.M., et al., 2015. Tensile properties of 420 mpa steel at low temperature. In: *The Twenty-Fifth International Ocean and Polar Engineering Conference*. International Society of Offshore and Polar Engineers.
- Tang, H., Fairchild, D., Panico, M., Crapps, J., Cheng, W., 2014. Strain capacity prediction of strain-based pipelines. In: *2014 10th International Pipeline Conference*. American Society of Mechanical Engineers V004T11A025–V004T11A025.
- P. Thomason, P. Thomason, *Ductile Fracture of Metals*.
- Tkaczyk, T., O’Dowd, N.P., Nikbin, K., Howard, B.P., et al., 2009. A non-linear fracture assessment procedure for pipeline materials with a yield plateau. In: *The Nineteenth International Offshore and Polar Engineering Conference*. International Society of Offshore and Polar Engineers.
- Tsuchida, N., Tomota, Y., Nagai, K., Fukaura, K., 2006. A simple relationship between Lüders elongation and work-hardening rate at lower yield stress. *Scr. Mater.* 54 (1), 57–60.
- Tu, S., Ren, X., He, J., Zhang, Z., 2018. Numerical study on the effect of the Lüders plateau on the ductile crack growth resistance of sent specimens. *Int. J. Fract.* 1–16.
- Tvergaard, V., 1981. Influence of voids on shear band instabilities under plane strain conditions. *Int. J. Fract.* 17 (4), 389–407.
- Tvergaard, V., 1982. On localization in ductile materials containing spherical voids. *Int. J. Fract.* 18 (4), 237–252.
- Tvergaard, V., Needleman, A., 1984. Analysis of the cup-cone fracture in a round tensile bar. *Acta Metall.* 32 (1), 157–169.
- Xia, L., Shih, C.F., 1995. Ductile crack growth-i. a numerical study using computational cells with microstructurally-based length scales. *J. Mech. Phys. Solids* 43 (2), 233–259.
- Zhang, Z., Niemi, E., 1994. A new failure criterion for the gurson-tvergaard dilatational constitutive model. *Int. J. Fract.* 70 (4), 321–334.
- Zhang, Z., Thaulow, C., Ødegård, J., 2000. A complete gurson model approach for ductile fracture. *Eng. Fract. Mech.* 67 (2), 155–168.